The Thesis Committee for Meredith Riley First
Certifies that this is the approved version of the following Thesis:

Characterization of a novel mouse model with adipocyte-specific disruption via the *aP2* promoter

APPROVED BY
SUPERVISING COMMITTEE:

Molly Bray, Supervisor

Laura Lashinger

Characterization of a novel mouse model with adipocyte-specific disruption via the *aP2* promoter

by

Meredith Riley First

Thesis

Presented to the Faculty of the Graduate School of

The University of Texas at Austin

in Partial Fulfillment

of the Requirements

for the Degree of

Master of Science in Nutritional Sciences

The University of Texas at Austin

May 2018

Abstract

Characterization of a novel mouse model with adipocyte-specific disruption via the *aP2* promoter

Meredith Riley First, MSNS

The University of Texas at Austin, 2018

Supervisor: Molly Bray

Circadian rhythms, the behavioral and physiological daily changes that occur in the majority of organisms, are partially generated via cell-autonomous molecular clock mechanisms. The functions of these molecular clocks vary with tissue and cell type. To examine clock function specifically within adipose tissue, a mouse model with a mutant *Clock* gene linked to the *aP2* promoter (*aP2* clock mutant, ACM) was created. The ACM model was verified with real-time quantitative PCR (qPCR) of mRNA levels for multiple circadian genes in several tissue types collected at different time points. These ACM mice were then assessed based on several physiological and behavioral parameters. Adult ACM animals weighed more ($F[14, 2657]=9.70$, $p<.001$) and have higher body fat percentages ($t[46]=-2.71$, $p<.01$) compared to wildtype animals. ACM mice exhibited increased food intake ($F[1,752]=5.23$, $p<.05$), higher respiratory exchange ratio ($F[1,524]=33.32$, $p<.001$), and higher energy expenditure ($F[1,524]=88.51$, $p<.001$), despite increased weight gain compared to wild-type mice. ACM animals also demonstrated higher levels of leptin

($F[1,28]=4.72$, $p<.05$) and non-esterified fatty acids ($F[1,29]=8.23$, $p<.01$). Tissue-specific disruption of the circadian clock appears to produce many of the phenotypes observed in global Clock mutant animals and suggests a critical role for tissues in which the aP2 promoter is active in regulating global metabolism and energy balance.

Table of Contents

Introduction 1

Materials and Methods 4

Animals 4

Dissections 4

Quantitative PCR 5

Growth and Hormone Measurements 5

Feeding Studies 5

GTTs 6

Metabolic Measures 6

Data Analysis 7

Results 8

Creation and Verification of the ACM Model 8

Effects of Genotype and Feeding on Body Composition 9

Effects of Genotype and Feeding on Glucose Tolerance 11

Analysis of Behavioral and Physiological Changes 11

Discussion 13

Figures 16

References 25

Introduction

The 24-hour day presents rhythmic, predictable patterns that include relatively static factors, such as the alteration between sunlight and darkness, as well as more variable, organism-dependent factors, such as meal timing and sleep cycles. The predictability of these patterns has led to the evolution of transcriptional molecular circadian clocks in almost all organisms, allowing for efficient cellular responses to repetitive environmental stimuli. Biological circadian rhythms are partially governed by these intrinsic transcriptional cellular clocks that are present in nearly all cell types. Rhythmic levels and frequency of expression of circadian genes and proteins influence transcription of downstream genes and execution of multiple cellular functions, including hormone release, metabolism, and behavior.[1,2]

The circadian clock is comprised of positive and negative feedback loops that depend upon the transcription, translocation, activity, and degradation of various circadian genes and proteins.[3] The main positive feedback loop is driven by the transcription and action of the *circadian locomotive output cycles kaput (Clock)* and *aryl hydrocarbon receptor nuclear translator-like (Arntl or Bmal1)* genes.[4] Once translated, CLOCK and BMAL1 proteins heterodimerize, translocate to the nucleus, and bind to E-box elements within the promoter regions of several genes, including the genes that encode them, thereby activating their own transcription.[3,5] Other clock genes include the *Period* family (*Per1, Per2,* and *Per3)*, *Cryptochrome* family (*Cry1* and *Cry2),* as well as *Retinoic acid orphan receptor alpha (Rora),* and *Nuclear receptor subfamily1 group D (Nr1d2 or Rev-erbα).*[3,5]

Once translated, PER and CRY proteins can also form a heterodimer (along with casein kinase I epsilon) and translocate to the nucleus, forming the negative loop of the clock mechanism that results in downregulation of the transcription of *Per* and *Cry* genes.[6] Degradation of PER and CRY proteins allows for the BMAL1/CLOCK heterodimer to again predominate, and the cycle begins again. Interactions of RORA and REV-ERBα form accessory positive and negative feedback loops, respectively. RORA enhances *Bmal1* transcription by interacting with ROR elements; conversely, interaction of REV-ERBα with ROR elements inhibits expression of *Bmal1*, which results in downregulation of its own expression.[7]

The circadian transcriptional mechanism is found nearly ubiquitously in all mammalian cells. Various investigations have been conducted in order to elucidate circadian clock function by inducing its disruption via genetic manipulation. Many transgenic animal models that disrupt circadian clocks do so indiscriminately, affecting all cells, and involve the alteration of global circadian gene expression. A widely studied model of circadian clock disruption is the dominant negative $Clock^{\Delta 19/\Delta 19}$ model, producing a *Clock* mutant gene that lacks the transactivation domain due to the loss of exon 19.[8,9] Mice with global $Clock^{\Delta 19}$ mutations have phenotypes characteristic of the metabolic syndrome, including obesity, hyperphagia, hyperleptinemia, hypoinsulinemia, hyperglycemia, and hyperlipidemia.[10]

Although the general components and mechanisms of the cellular clock are the same across cell types, the functions of cell-specific clocks have been shown to vary.[11,12] Because increased adiposity and metabolic dysfunction are central to global $Clock^{\Delta 19}$

mutant animals, we created a tissue-specific mouse model in which the *Clock*$^{\Delta 19}$ mutation is driven by the fatty acid-binding protein 2 (*aP2)* promoter, which is predominantly active in adipocytes. The mutated dn*Clock* gene is highly overexpressed in this aP2 Clock Mutant (ACM) model, causing the dnCLOCK protein to preferentially bind to BMAL1 over the endogenous CLOCK, thereby creating a non-functional heterodimer and a resultant tissue-specific disrupted circadian cycle. This mouse model shows circadian disruption in primarily adipose tissue and does not exhibit whole body circadian disruption, allowing for a more detailed examination of the function of the cellular clock within adipocytes. Here we report the primary phenotypes associated with the ACM animal model.

Materials and Methods

Animals

Both ACM mice and wild-type (WT) littermates on the FVB/N background were housed at the Children's Nutrition Research Center at Baylor College of Medicine or at the Center for Comparative Medicine at the University of Alabama at Birmingham. All studies and protocols were approved by their respective Institutional Animal Care and Use Committees. Mice were housed in standard micro-isolator cages (except during feeding studies, during which they were housed on wire-bottom cages or within a Comprehensive Lab Animal Monitoring System (CLAMS)), within a controlled environment, including a 12:12 hour light-dark cycle with temperature maintained at 23±1°C. Food and water were provided *ad libitum,* unless otherwise specified. Transgenic ACM mice were created via pronuclear injection of a dn*Clock* construct lacking exon 19 that was driven by the *aP2* promoter. The *aP2* promoter is primarily expressed in adipocytes; however, it has also been shown to have low activity in macrophages, dendritic cells, and cardiomyocytes.[13] Genotypes were verified using the following primers: 5'-ATTGTTCACTCCTACAGTCAC and 5'-CCAGGAAGCATAGACCCCAGC.

Dissections

Male ACM and WT mice were anesthetized with pentobarbital prior to drawing of blood and subsequent removal of the heart, liver, adipose tissue (peri-gonadal, subcutaneous, and brown), and muscle (gastrocnemius) samples. Tissues were dissected every 3 hours for 24 hours. During dissections, zeitgeber time (ZT) conditions were maintained, with ZT0 defined as the time lights were turned on and ZT12 as the time lights turned off.

Quantitative PCR

qPCR was performed using methods previously described.[14-16] qPCR data are represented as mRNA molecules per microgram of total RNA. Primer and probe sequences for *Bmal1* and *Clock* have been published previously.[16]

Growth and Hormone Measurements

Daily food intake was monitored manually during feeding protocols. Body weights were measured weekly. Body composition measures were performed in mice 5-6 months of age using a Lunar PIXImus Densitometer (GE Medical Systems, Madison, WI). Non-fasted plasma glucose, non-esterified fatty acids, insulin, triglycerides, and leptin concentrations were measured using commercially available kits (Thermo Scientific, Waltham, MA; Wako Diagnostics, Richmond, VA; CrystalChemInc., Downers Grove, IL; Linco Research, Inc., St. Charles, MO).

Feeding Studies

Mice were fed either a standard chow (Harlan, cat. No. Teklad 7917), a low fat (10% kcals fat, LF, Research Diets, D12450B), a high fat (45% kcals fat, HF, Research Diets, D12451), or a very high fat (60% kcals fat, VHF, Research Diets, D12492) diet. All non-standard diets were matched for protein content and macronutrient quality. Access to food was either *ad libitum* or a specialized protocol was used to simulate "meals" of different compositions presented at distinct times during the active phase (ZT12-ZT24). This phase was divided into three four-hour time periods, and four-hour "meals" were provided at the beginning (ZT12-ZT16) and end (ZT20-ZT24) of the active phase, separated by 4 hours (ZT16-ZT20) of food restriction. The feeding paradigm consisted of

either a HF/VHF waking "meal" (ZT12-ZT16) combined with a LF "meal" during the last 4 hours of the waking period (ZT20-ZT24), or the opposite meal order.

GTTs

Glucose tolerance tests (GTT) were performed for the three experimental feeding protocols. GTTs were performed at 6, 10, 12, and 20-23 weeks of age. Prior to each GTT, animals were fasted for 10 hours. Tails were nicked, and baseline plasma glucose measurements were taken using a Freestyle glucometer. Animals were injected intraperitoneally with 10% D-glucose (0.01 ml/g). Plasma glucose levels were measured at 15, 30, 60, 90, and 120 minutes after injection.

Metabolic Measures

ACM and WT mice were placed into individual cages in a Comprehensive Lab Animal Monitoring System (CLAMS) for one week. Throughout the week, lights were turned on at 8 am (ZT0) and turned off at 8 pm (ZT12), and temperature was maintained at 25±1.5°C. After a three-day acclimation period, the CLAMS recorded data on respiratory exchange ratio (RER), energy expenditure (EE), food intake, and physical activity (measured by beam breaks along two planes). Data were recorded every 15 minutes and were categorized into light (ZT0-ZT12) or dark (ZT12-ZT24) time periods. Food intake and movement were summed across these time periods per day and averaged across days. EE and RER were averaged per time period, then averaged across days.

Data Analysis

Unless otherwise specified, all statistical analyses were performed using StataSE 13 (StataCorp, College Station, TX). The area under the curve (AUC) was determined for GTTs. Analysis of covariance (ANCOVA) was used to determine main effects and interactions, and significant results were followed with *post hoc* tests using the Bonferroni correction method in order to maintain a family-wise error rate of $p<0.05$. Cosinor analyses were performed to examine rhythmicity of gene expression and metabolic data.

Results

Creation and Verification of the ACM Model

In order to verify the ACM model, various tissues were collected from mice at a single ZT point, and qRT-PCR was performed on *Clock* mRNA. Results include both endogenous *Clock* and *dnClock* mRNA (Figure 1). No significant differences were observed between WT and ACM animals in kidneys or in livers. In all of the tissues with differential *Clock* expression, ACM mice had greater *Clock*+*dnClock* mRNA than WT animals. In muscle and heart tissue, expression of *Clock*+*dnClock* mRNA was approximately two-fold higher in the ACM mice (muscle: 529±233; heart: 787±50, $p<0.05$) compared to WT mice (muscle: 152±40; heart: 393±14). On the other hand, *Clock*+*dnClock* expression levels in subcutaneous tissue (SAT) and visceral fat (VAT) of ACM mice were 13-24 fold higher than those of WT mice (SAT: 4933±2190; VAT: 4002±1857 vs. SAT: 201±56; VAT: 315±80, respectively, $p<0.05$).

In order to examine clock genes over time, qRT-PCR was performed for the circadian genes *Clock* and *Bmal1* in white and brown adipose tissue across eight ZTs, each three hours apart (Figure 2). Analyses revealed a significant effect between genotypes for *Clock*+*dnClock* ($F(7,59)=102.51$, $p<.001$) with ACM mice having constitutively higher levels of *Clock* mRNA (3315±1715) than WT mice (423±165). Due to their oscillatory nature, a significant main effect of ZT was seen for *Bmal1* ($F(7,57)=8.62$, $p<.001$), but no such main effects were apparent between genotypes for *Bmal1* ($F(5,57)=0.46$, $p>.05$). Because ACM mice appeared to have an advance in peak expression of *Bmal1* compared to WT (ZT 18 vs. ZT 24, respectively), cosinor analysis was performed to test for a

significant phase advance in ACM *Bmal1* expression. Based on R-squared values, a non-linear model explained approximately 45% of the variance in WT compared to 47% of the variance in ACM mice. Parameters of the model were not significantly different between genotypes.

Effects of Genotype and Feeding on Body Composition

Because the disruption of clocks in ACM animals is primarily localized to adipocytes, total body weight and adiposity were examined (Figure 3). At five months of age, ACM mice had higher fat percentages than WT mice (22.1±4.3 % vs.17.8±3.8 %, respectively; $p>0.05$). In 10-month-old mice, there were no differences in total body weight, but there were significant differences in body fat ($t(46)=-2.71$, $p<.01$); again, ACM mice had significantly higher fat percentages than WT mice (29.6±9.8 vs. 23.6±5.0, respectively).

To test for trends in weight gain between ACM and WT mice, monthly body weight data were compared in mice that had not been used in any experiments, had lived to at least one year of age, and had been weighed at least once per month (Figure 4). A significant main effect of genotype ($F(1, 173)=10.51$, $p<.01$) and a main effect of age ($F(16, 2657)=2601$, $p<.001$), as well as an interaction of genotype and age ($F(14, 2657)=9.70$, $p<.001$) were all observed.

To examine whether these differences in body weight were associated with food intake, young male mice were fed either LF or HF diets, matched for protein intake, for one month. At three to four months of age, body fat and total weight were measured (Figure

5). For body fat, a main effect was seen both for diet ($F(1,12)=10.61$, $p<.01$) and for genotype ($F(1,12)=5.92$, $p<.05$), with ACM mice and those fed high fat chow having higher adiposity measures.

Based on our previous work demonstrating that timing of feeding is important in metabolic response to high fat diets, ACM and WT mice were exposed to the feeding schedule consisting of two 4-hour "meals" at the beginning and end of the waking period, one during which they were given either HF or VHF food, and the other during which they were given LF chow. After 15 weeks on this feeding schedule, body composition and weight measures were assessed (Figure 6). Groups were categorized based on genotype (ACM vs. WT), diet (HF and LF vs. VHF and LF), and timing of access to the high fat chow (early vs. late). Total body weight showed a main effect of genotype ($F(1,39)=5.30$, $p<.05$). ACM mice tended to have higher weight overall (38.4±4.0 g) than WT mice (38.4±4.0 g) (36.1±3.2 g), with the effect being especially apparent for the late very high fat feeding group, in which ACM mice weighed over five grams more (41.2±2.6 g) than WT mice (34.7±3.9 g).

Body fat percentage also showed a main effect of genotype ($F(1,39)=8.59$, $p<.01$). Consistent with the patterns in weight, ACM mice had higher fat (34.0±5.1%) than WT mice (30.3±3.8%) overall, but this difference was especially apparent for those given late access to very high fat chow, with ACM mice having a higher percent fat (37.1±3.5 %) than WT mice (28.0±5.1 %).

Effects of Genotype and Feeding on Glucose Tolerance

In WT and ACM mice at 6-7, 10, 13-14 and 20 weeks of age fed standard chow *ad libitum*, there were no significant differences observed between genotype groups in AUC or glucose values over time at any age.

For animals in the EVHF and EHF groups that were fed according to the 4-hour "meal" paradigm, no significant genotype difference was observed in AUC or in glucose over time (Figure 7 A&C). In the late fat groups (LVHF and LHF), a significant genotype difference was observed in glucose values over time (Figure 7 B&D LVHF: 232.78±8.62 mg/dl vs. 283.19±14.54 mg/dl LHF: 245.40±14.62 mg/dl vs. 282.81±12.94 mg/dl; WT and ACM, respectively).

Analysis of Behavioral and Physiological Changes

In order to explore potential causes for the discrepancies in weight and body fat between WT and ACM mice, eight of each genotype were placed into a CLAMS to determine daily trends for food intake, activity, energy expenditure (EE), and respiratory exchange ratio (RER). Collected data was divided into three-hour time periods. Food and movement were totaled for each time period, while EE and RER were averaged (Figure 8).

A main effect of genotype was seen for food intake ($F(1,752)=5.23$, $p<.05$), with ACM mice eating more than WT mice overall. There was also a main effect of time period on food intake ($F(7,752)=14.87$, $p<.001$) (Figure 8A). Activity did not show a main effect of genotype, but did exhibit a main effect for time period ($F(1,524)=19.02$, $p<.001$) (Figure 8C). RER had significant main effects of both time period ($F(7,524)=14.54$, $p<.001$) and

genotype ($F(1,524)=33.32$, $p<.001$), with ACM mice showing more energy utilization from carbohydrate versus fat metabolism than WT mice (Figure 8B). EE showed a main effect for both time period ($F(1,524)=41.98$, $p<.001$) and genotype ($F(1,524)=88.15$, $p<.001$), with ACM mice exhibiting greater expenditure than WT mice (Figure 8D).

To further examine potential contributors to the increases in body fat and weight seen in ACM mice, several blood analytes, including leptin, cholesterol, non-esterified fatty acids (NEFA), and triglycerides, were analyzed (Figure 9). These analytes were measured through blood samples collected at four different ZT points. No significant effects of genotype or time were seen for cholesterol or for triglycerides (Figures 9A and 9B). For leptin, a main effect of genotype was apparent ($F(1,28)=4.72$, $p<.05$), with ACM mice having higher average levels (14.2±13.3 ng/ml) of leptin than WT mice (5.8±3.5 ng/ml), with a striking surge of leptin at ZT18 (Figure 9C). Main effects of both genotype ($F(1,29)=8.23$, $p<.01$) and time ($F(5,29)=3.73$, $p<.01$) were apparent for NEFA levels. NEFA levels tended to be higher in ACM mice (0.25±.09 mE/L) than in WT mice (0.20±.05 mE/L) (Figure 9D).

Discussion

The creation of an adipocyte specific circadian disruption model was achieved via a dominant negative *Clock* gene lacking the normal transactivation domain, the transcription of which is linked to the *aP2* promoter. This model was verified by the significant overexpression of *Clock* mRNA seen primarily in fat tissues. Although 24-hour disruption of *Bmal1* was not apparent, this observation could be due to maintained rhythmicity of non-adipocyte cell types within the sample. The significance of a phase advance in peak *Bmal1* is not known.

ACM mice fed normal chow tended to weigh more than their WT counterparts, a trend that was exacerbated after the animals reached adulthood (approximately 3 months of age). Differences in adiposity were more profound and also appeared to be exaggerated with age, with adult ACM mice having higher body fat than WT animals. The results seem to mimic phenotypes observed in global knockouts, although to a lesser extent.[10] These effects on body weight and body composition were not highly influenced by a change in the fat content of diet, as both genotypes seemed to increase the same amount of weight and body fat due to the increase in fat intake. However, the introduction of a varied diet and an even higher fat chow did elicit markedly different responses between the two genotypes. ACM mice were particularly sensitive to a timed feeding regimen that included exposure to very high fat meal at the end, but not the beginning, of their active period. With exposure to normal chow diets, ACM mice demonstrated higher food intake, as well as higher RER, indicating increased reliance on energy from carbohydrate metabolism than stored fat metabolism. The difference in RER between genotypes trended toward an

interaction with time, and reliance on carbohydrate metabolism appeared to be especially apparent toward the end of the dark period. In addition, ACM mice tended to have higher energy expenditure than WT mice, although there were no differences in activity levels detected between genotypes.

The adipokines measured (leptin, cholesterol, triglycerides, and NEFAs) were all associated with the amount and activities of adipose tissue. Leptin is a hormone that acts as a satiety signal, and therefore, is implicated in the regulation of body weight and energy balance.[17] High levels of serum cholesterol are associated with overweight/obesity and atherosclerotic risk.[18,19] High triglycerides are associated with insulin resistance, cardiovascular disease, and metabolic syndrome.[20] NEFAs are fatty acids that can be synthesized endogenously by the organism, and levels are elevated in obesity.[21] Interestingly, leptin levels of ACM mice spiked at later time points (ZT18) of the dark period, concomitant with observed increases in food intake at this phase. This incongruous pairing of increased intake despite elevated satiety signaling may indicate a time-dependent leptin resistance in ACM mice, leading to impaired metabolism in the late phase and their metabolic syndrome-like phenotype. The observed increases in NEFA corroborate this hypothesis, signaling a time-dependent impairment of fat metabolism in the ACM mice. Though there were no evident defects in glucose tolerance in the ACM animals, the differences in EE, RER, and leptin levels observed with adipocyte clock disruption have implications in energy balance outcomes.

The collection of these data suggests that several aspects of the metabolic

syndrome-like phenotype observed in animals with global *Clock* disruption are at least partially attributable to disruption specifically within adipocytes. Continued examination of the physiological differences of ACM mice both at baseline and after dietary manipulations is warranted to elucidate the roles of the circadian clock in adipocytes.

Figures

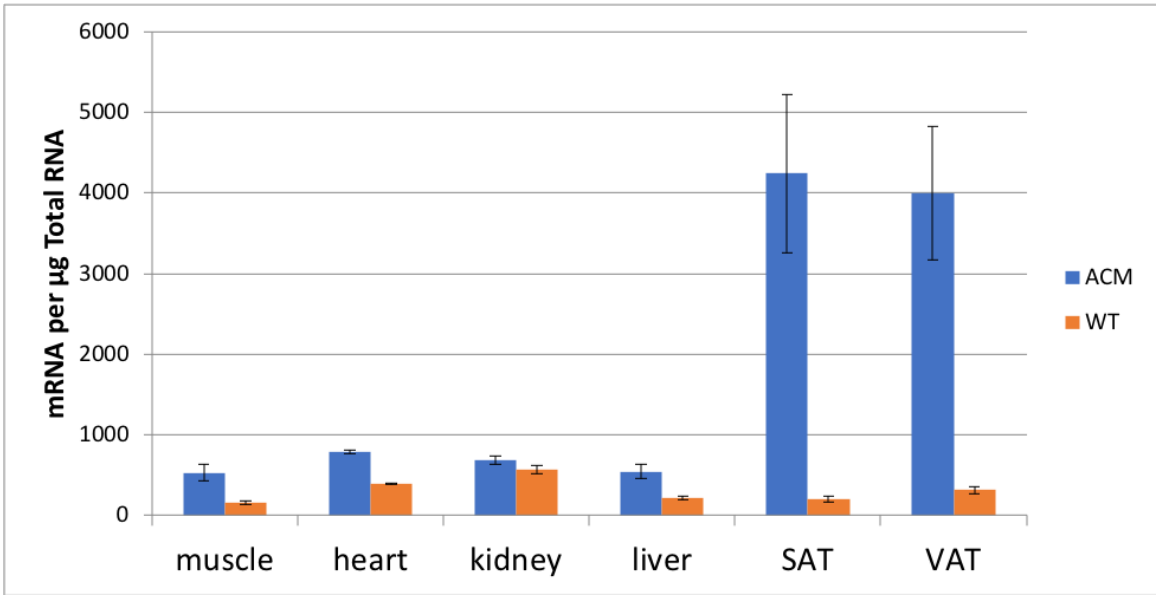

Figure 1: qRT-PCR for *Clock+dnClock* in various tissues. Significant differences in *Clock+dnClock* mRNA levels were observed in gastrocnemius (muscle), heart, subcutaneous tissue (SAT), and visceral fat (VAT). Compared to other tissues, the adipocyte-derived tissues have significantly higher *Clock+dnClock* expression.

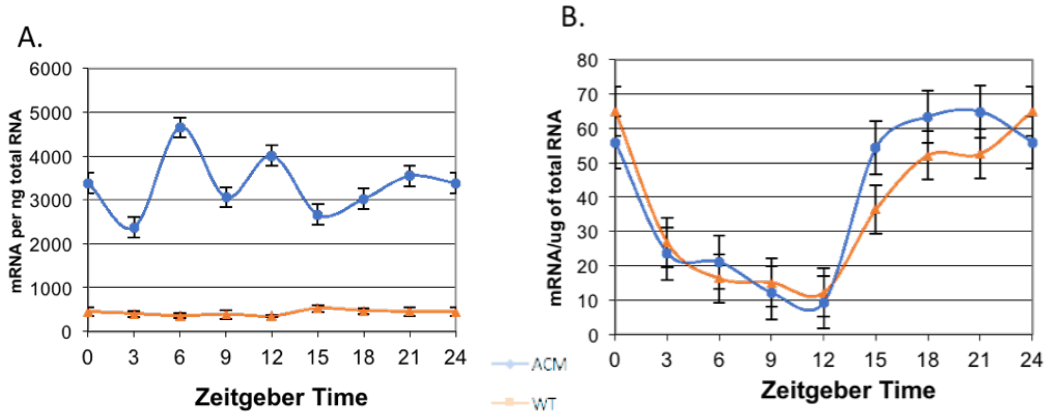

Figure 2: qRT-PCR for A. *Clock+dnClock* and B. *Bmal1* in white adipose tissue. A main effect of genotype was seen for *Clock+dnClock* mRNA levels. No significant main effects or interactions involving genotype were present in *Bmal1* mRNA.

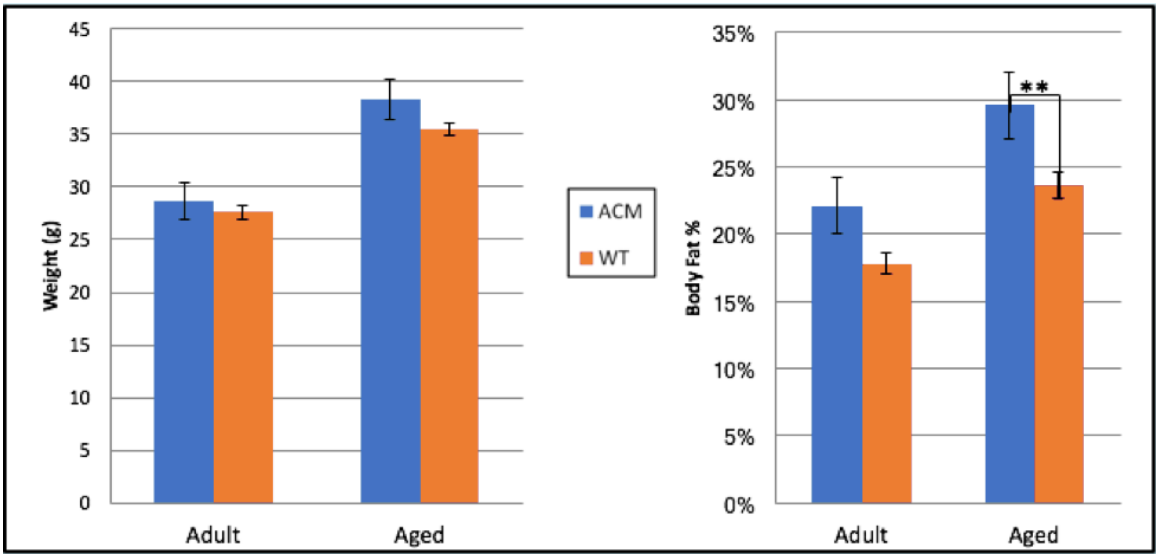

Figure 3: A. Body weight and B. body fat measures in adult (5-6 months) and aged (10 months) animals of each genotype. No differences were seen between genotypes for total body weight of male mice approximately five months of age. The difference in body fat percentage was trending toward significance; $t(23)=-2.03$, $p=.054$; with ACM mice showing slightly higher body fat than WT mice.

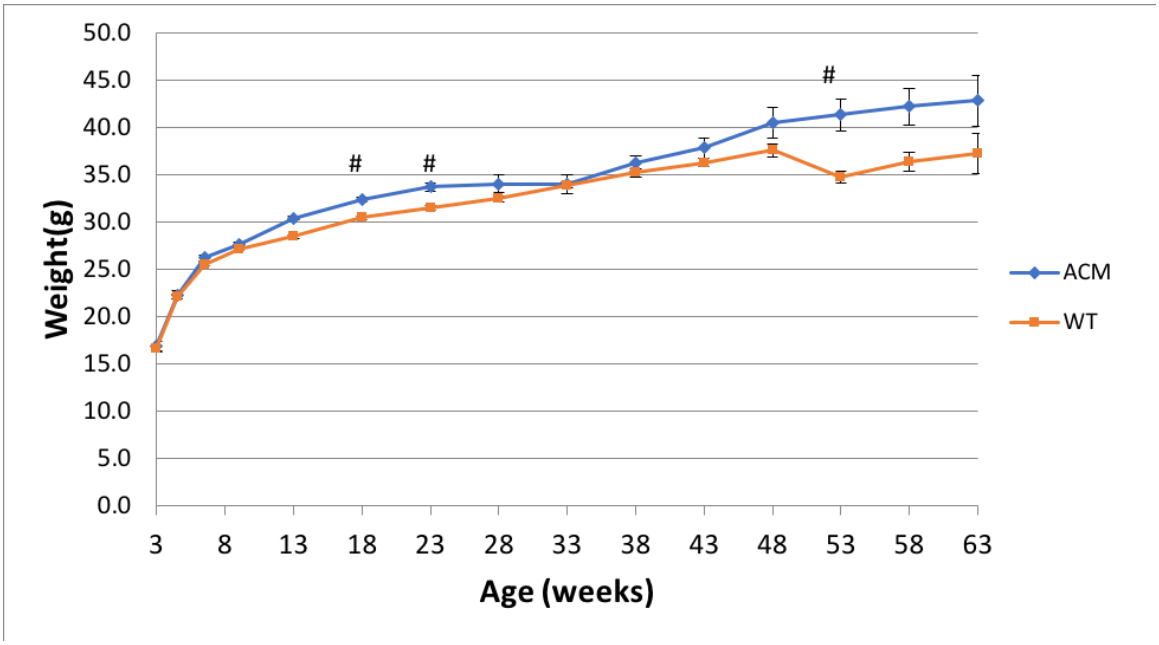

Figure 4: Weight comparisons of ACM and WT mice. Weight data were collected from male mice >1 year of age who had not undergone any other experimental procedures and had only been given standard chow *ad libitum*. A significant main effect was seen for both genotype and age, as well as an interaction between the two. The *post hoc* tests per age group revealed significant differences being maintained in four of the fifteen age segments. #=p_{FW}<.05, ***=p<.001.

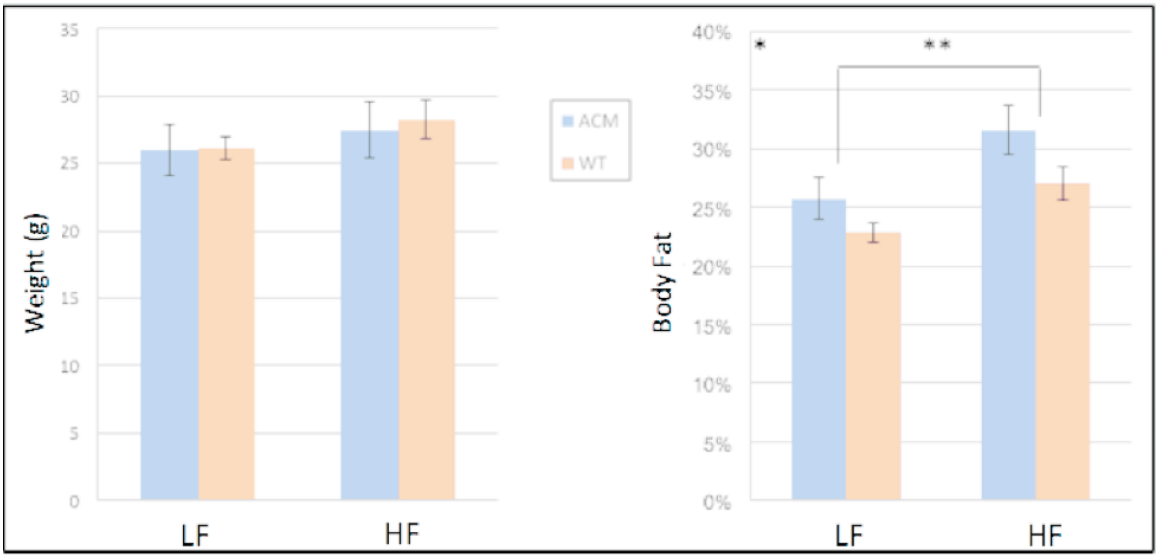

Figure 5: A. Body weight and B. body fat measures in ACM and WT mice fed LF or HF chow *ad libitum*. No significant effects for body weight were seen for diet or genotype. Main effects of genotype ($p<.05$) and diet ($p<.01$) were seen for body fat percentage, with the high fat diet and ACM genotype being associated with higher body fat. *=$p<.05$, **=$p<.01$.

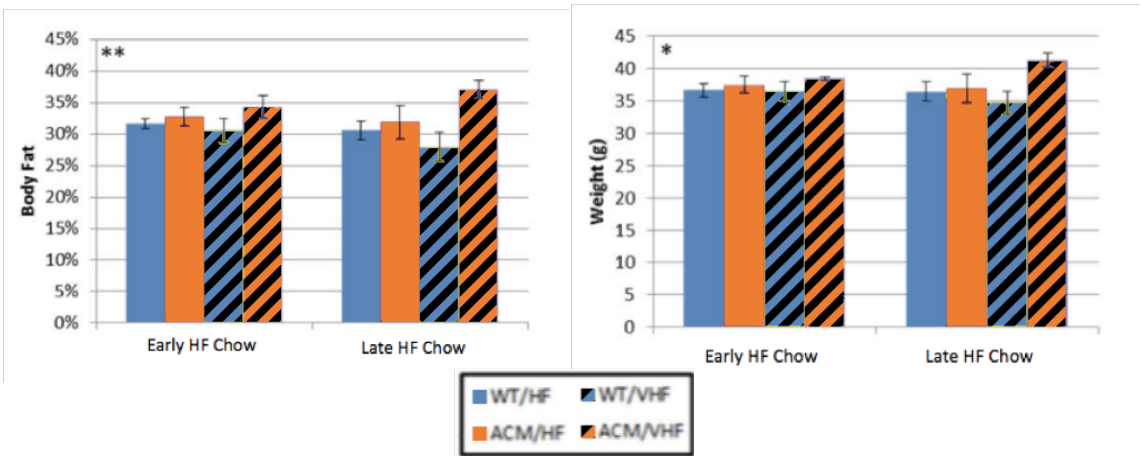

Figure 6: A. Body weight and B. body fat measures in ACM and WT mice fed two 4-hour "meals" separated by a 4-hour phase of food restriction for 15 weeks. Mice were fed a combination of high fat (HF) or very high fat (VHF) in combination with low fat food. They were given early access to one food type during the first four hours of their dark period (ZT12-16), and late access to the other food type during the last four hours of dark (ZT20-24). Groups are divided by timing of access to the fatty chow (HF or VHF), genotype, and which high fat chow was received. A main effect of genotype was seen for weight, with ACM mice showing higher weight than WT mice (A). Similar results were seen for body fat, with a main effect for genotype, and ACM mice having higher body fat than WT mice (B). *=p<.05, **=p<.01.

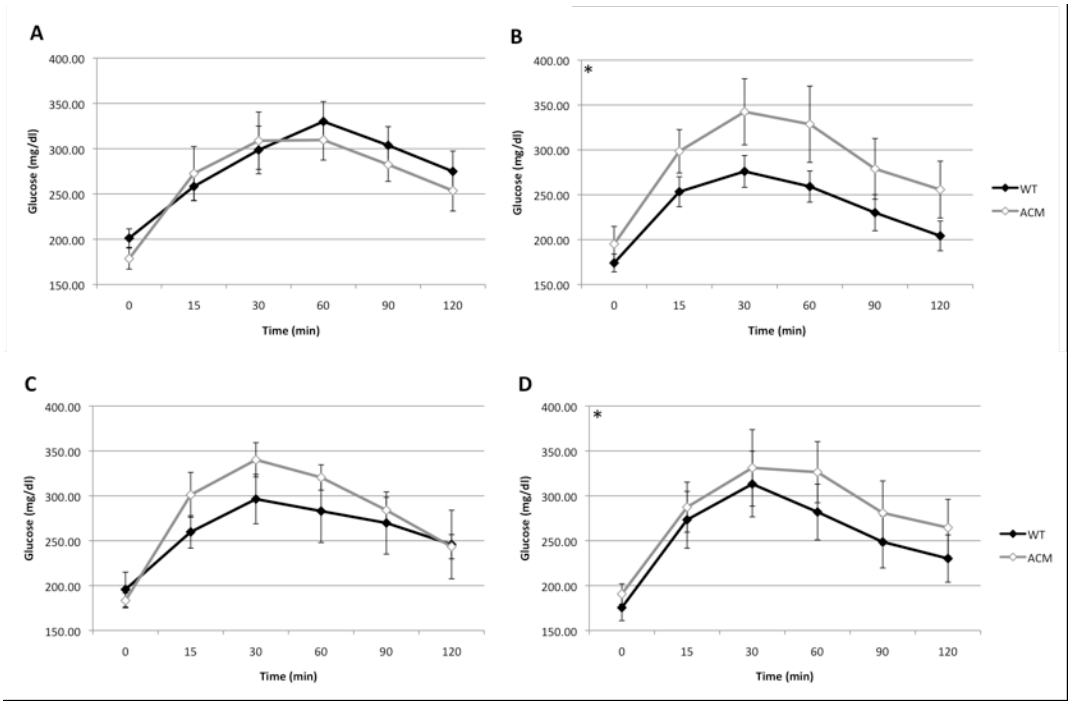

Figure 7: GTT results by Genotype post-short-term time restricted feeding: A. EVHF B. LVHF C. EHF D. LHF. Results shown as mean +/- sem. *genotype effect $p<0.05$

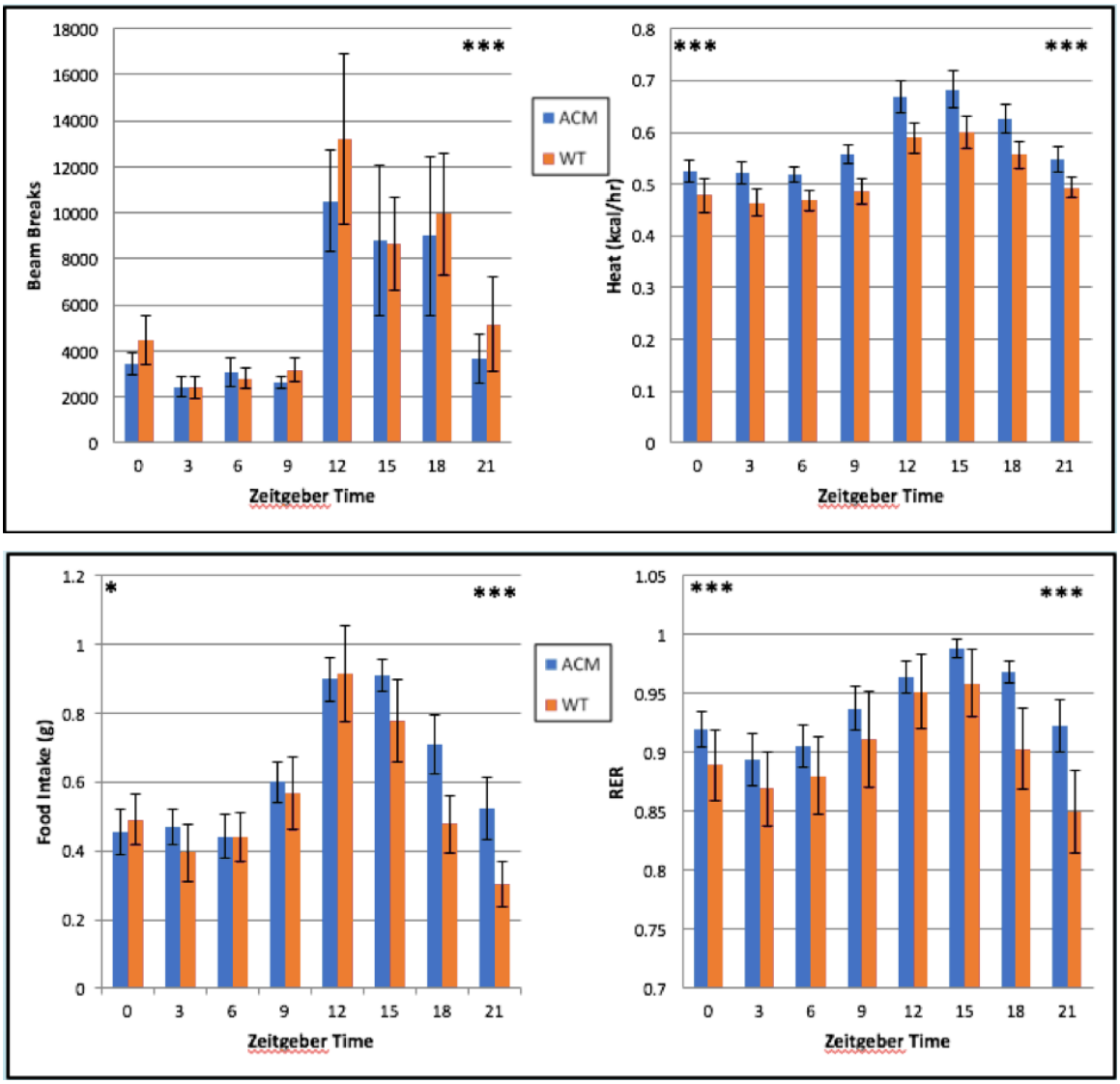

Figure 8: CLAMS behavioral and physiological measures in ACM and WT mice. Data were recorded for A. food intake, B. respiratory exchange ratio (RER), C. activity, and D. energy expenditure (EE). The data were divided into three-hour segments. Food intake and movement values were summed across these periods, while RER and EE were averaged. Main effects of genotype and Zeitgeber time (ZT) for food intake were observed, with ACM mice eating more than WT mice. There were main effects of genotype and ZT for RER, as well as a trend toward an interaction ($F[7,524]=1.97$, $p=.057$). RER values were closer to 1.0 in ACM animals, indicative of greater reliance on carbohydrate metabolism than stored fat metabolism compared to WT mice. No main effect of genotype, but a main effect of ZT, was observed for activity. A significant main effect of genotype was observed with EE, with ACM mice having higher EE values than WT mice overall. *=$p<.05$, ***=$p<.001$.

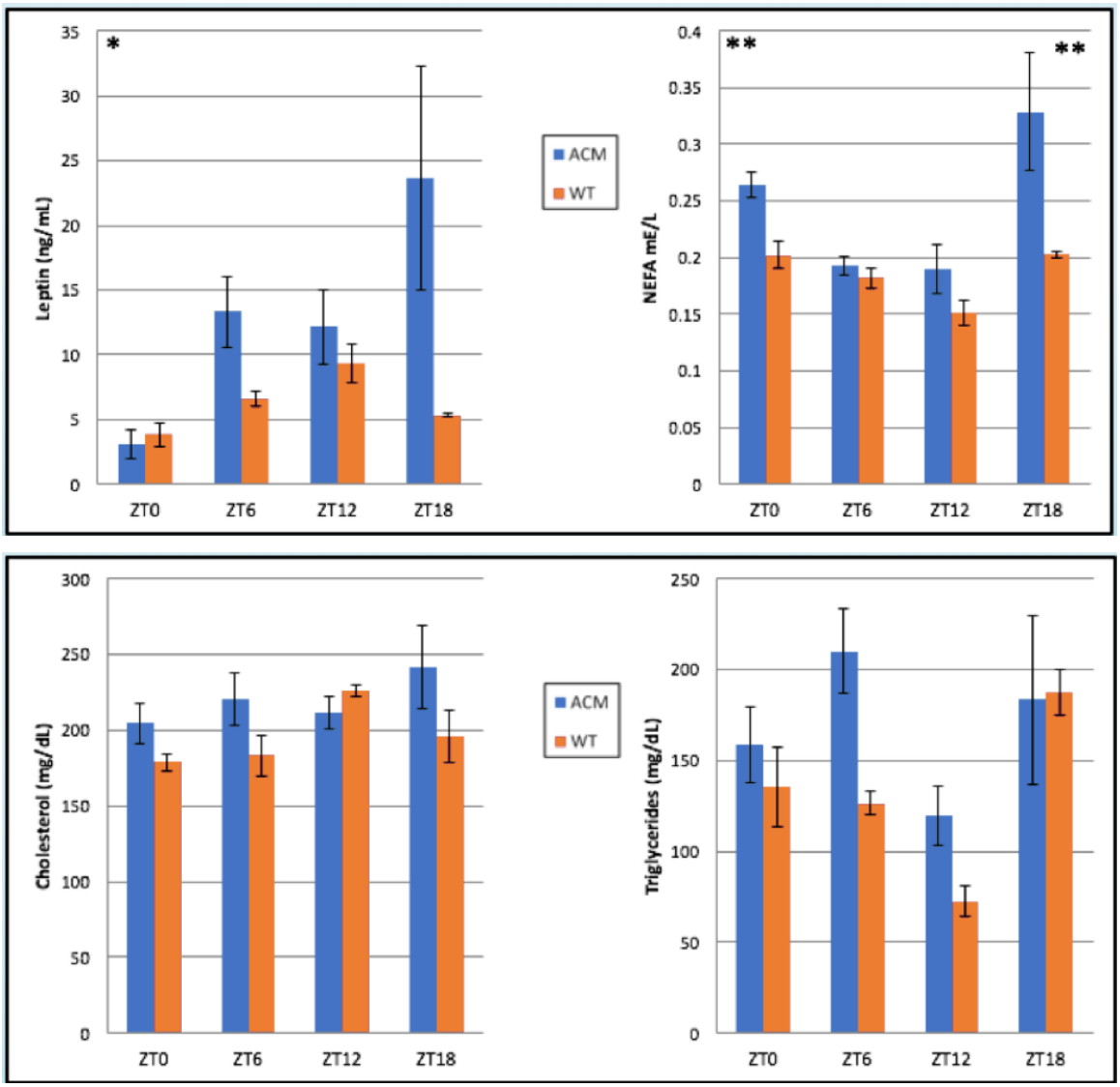

Figure 9: Adipokine levels at four different ZT points. No main effects of genotype or time for A. cholesterol or B. triglycerides were observed. C. ACM animals had higher leptin levels compared to WT. D. Main effects of genotype and time were observed for NEFA levels. *=p<.05, **=p<.01.

References

1. Hastings M, O'Neill JS, Maywood ES. Circadian clocks: regulators of endocrine and metabolic rhythms. *The Journal of endocrinology*. 2007;195(2):187-198.
2. Kohsaka A, Laposky AD, Ramsey KM, et al. High-fat diet disrupts behavioral and molecular circadian rhythms in mice. *Cell metabolism*. 2007;6(5):414-421.
3. Takahashi JS. Molecular components of the circadian clock in mammals. *Diabetes, obesity & metabolism*. 2015;17 Suppl 1:6-11.
4. Lande-Diner L, Boyault C, Kim JY, Weitz CJ. A positive feedback loop links circadian clock factor CLOCK-BMAL1 to the basic transcriptional machinery. *Proceedings of the National Academy of Sciences of the United States of America*. 2013;110(40):16021-16026.
5. Kondratov RV, Gorbacheva VY, Antoch MP. The role of mammalian circadian proteins in normal physiology and genotoxic stress responses. *Current topics in developmental biology*. 2007;78:173-216.
6. Duong HA, Robles MS, Knutti D, Weitz CJ. A molecular mechanism for circadian clock negative feedback. *Science (New York, NY)*. 2011;332(6036):1436-1439.
7. Guillaumond F, Dardente H, Giguere V, Cermakian N. Differential control of Bmal1 circadian transcription by REV-ERB and ROR nuclear receptors. *Journal of biological rhythms*. 2005;20(5):391-403.
8. King DP, Zhao Y, Sangoram AM, et al. Positional cloning of the mouse circadian clock gene. *Cell*. 1997;89(4):641-653.

9. Vitaterna MH, King DP, Chang AM, et al. Mutagenesis and mapping of a mouse gene, Clock, essential for circadian behavior. *Science (New York, NY)*. 1994;264(5159):719-725.

10. Turek FW, Joshu C, Kohsaka A, et al. Obesity and metabolic syndrome in circadian Clock mutant mice. *Science (New York, NY)*. 2005;308(5724):1043-1045.

11. Bray MS, Young ME. The role of cell-specific circadian clocks in metabolism and disease. *Obesity reviews : an official journal of the International Association for the Study of Obesity*. 2009;10 Suppl 2:6-13.

12. Ramanathan C, Xu H, Khan SK, et al. Cell type-specific functions of period genes revealed by novel adipocyte and hepatocyte circadian clock models. *PLoS genetics*. 2014;10(4):e1004244.

13. Makowski L, Boord JB, Maeda K, et al. Lack of macrophage fatty-acid-binding protein aP2 protects mice deficient in apolipoprotein E against atherosclerosis. *Nat Med*. 2001;7(6):699-705.

14. Gibson UE, Heid CA, Williams PM. A novel method for real time quantitative RT-PCR. *Genome research*. 1996;6(10):995-1001.

15. Heid CA, Stevens J, Livak KJ, Williams PM. Real time quantitative PCR. *Genome research*. 1996;6(10):986-994.

16. Bray MS, Shaw CA, Moore MW, et al. Disruption of the circadian clock within the cardiomyocyte influences myocardial contractile function, metabolism, and gene expression. *American journal of physiology Heart and circulatory physiology*. 2008;294(2):H1036-1047.

17. Paz-Filho G, Mastronardi CA, Licinio J. Leptin treatment: facts and expectations. *Metabolism: clinical and experimental*. 2015;64(1):146-156.

18. Hansson GK, Libby P. The immune response in atherosclerosis: a double-edged sword. *Nature reviews Immunology*. 2006;6(7):508-519.

19. Glass CK, Witztum JL. Atherosclerosis. the road ahead. *Cell*. 2001;104(4):503-516.

20. Joseph J, Shamburek RD, Cochran EK, Gorden P, Brown RJ. Lipid regulation in lipodystrophy versus the obesity-associated metabolic syndrome: the dissociation of HDL-C and triglycerides. *The Journal of clinical endocrinology and metabolism*. 2014;99(9):E1676-1680.

21. Reddy NL, Peng C, Carreira MC, et al. Enhanced thermic effect of food, postprandial NEFA suppression and raised adiponectin in obese women who eat slowly. *Clinical endocrinology*. 2015;82(6):831-837.